



## **DRAG ANALYSIS OF THREE RUDDER-SHAPED LIKE BODIES**

M. N. Azzeri<sup>1 2 3</sup>, O. E. Hanis<sup>1 2</sup>, Adi Maimun<sup>1 2</sup>, F. A. Adnan<sup>4</sup>, P. A. Wilson<sup>5</sup>  
and M. Z. Md. Zain<sup>1</sup>

<sup>1</sup>School of Mechanical Engineering,  
Universiti Teknologi Malaysia,  
81210 Skudai, Johor Bahru

<sup>2</sup>Marine Technology Center,  
Universiti Teknologi Malaysia,  
81210 Skudai, Johor Bahru

<sup>3</sup>Faculty of Science & Defence Technology,  
Universiti Pertahanan Nasional Malaysia,  
57000 Kuala Lumpur, Malaysia

<sup>4</sup>Marine Cons. & Maintenance Tech.,  
Malaysian Institute of Marine Engineering Technology,  
32200 Lumut, Malaysia.

<sup>5</sup>Fluid-Structure Interactions Research Group,  
Faculty of Engineering and the Environment University of Southampton,  
Burgess Road, Southampton, United Kingdom.

### **ABSTRACT**

*This paper presents an investigation of Rudder Shaped-Like (RSL) hull configurations with low-drag characteristic using the resistance model tests and numerical analysis. The new design of the floating platform using three hulls with a self-manoeuvring system as Unmanned Surface Vehicle (USV) and capable of collecting the same data as a hydrography boat is needed. This platform was designed with three hulls placed in a triangle position in the form of rudder shape and vertically placed as a slender body shape using NACA 0012 profile. This provides the low-drag characteristic to USV. The results from the experimental and numerical analysis revealed that a larger configuration distance between three hulls leads to a reduction in resistance of the same speed. This result may help to accomplish the required concept design related to low-drag and minimum power operation.*

**Keywords :** *Rudder shaped-like, Unmanned Surface Vehicle, Resistance*

### **1.0 INTRODUCTION**

The new design of floating platform using three hulls with a self-manoeuvring system as Unmanned Surface Vehicle (USV) and capable of collecting the same data as a hydrography boat is needed. This new platform provides moderate speed with long

---

\*Corresponding author: [azzerinaiem@yahoo.com](mailto:azzerinaiem@yahoo.com)

endurance and is kept in station at the one reference point for ocean measurement activities such as recording wave data, meteorological data, current data, sea surface data, and other oceanographic measurements with improved capabilities of resistance and seakeeping [1].

Investigations into the resistance of three hulls or trimaran have proven that such hull forms have lower resistance at high speeds when compared with catamarans and mono hull of similar displacement [2]. In recent years, the term trimaran has been associated with a vessel made of three hulls with a larger central main hull and two smaller side hulls called the outriggers. Another term of a vessel made of three-hull is Tricore but it is different from the trimaran because it is a vessel which are made of three identical hulls of the same shape [3]. The study of rudder-shaped like (RSL) is similar to the Tricore to increase the speed of a vessel with corresponding reduction in required power.

Ship resistance is the force required to move it in calm water at constant velocity and considered as one of the important factors in designing the ship. Most previous research has focused on methods employed to determine the resistance of each trimaran model on simulation studies comprise computational fluid dynamic (CFD) and model test experimental investigation. The use of CFD to determine ship resistance is not new as it consume less time [4]. Furthermore, CFD allows ship designers to simulate the model of a ship at various speeds, thus it is much easier to understand the complicated flow around the hull. However, the simulation studies still lack support and verification from real experimental data. Furthermore, if the research is conducted using simulations and experiment, the results obtained are validated with experimental data. The simulation results are in good agreement with the experimental data.

Therefore, this study presents an investigation of RSL hull configurations with low-drag characteristic that uses resistance model tests and CFD codes. In ship hydrodynamics, drag is also named “resistance” [5]. This allows the study to determine if the total resistance of the RSL platform is at an acceptable level. Other than that, the positions of the hulls are very important in order to optimise their performance [6]. This RSL design uses three RSL bodies in columns with NACA 0012 profile hull form for low-drag determination.

## 2.0 HULL FORM AND THREE HULL CONFIGURATIONS

The basic concept of this RSL model platform of the design is the combination of three identical hulls (tricore) with NACA 0012 profiles as shown in Figure 1. This model operates in low speed. In fact, the three hulls for trimaran types are usually faced with a high resistance at a low speed due to large wetted surface area, which are affected by the high percentage of frictional resistance [7]. By using NACA profile shape that provides the model with low-drag characteristic, minimum power requirements are needed in manoeuvring and station-keeping. Table 1 shows the particulars of the RSL model.

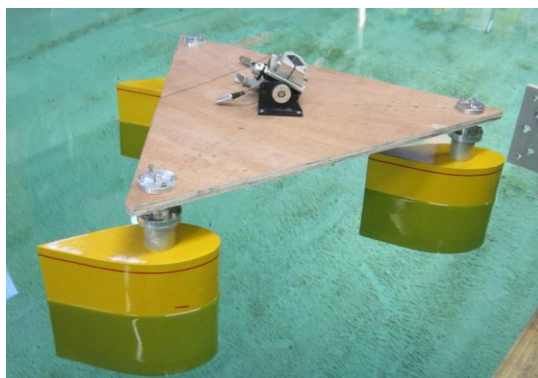


Figure 1: Model design RSL.

Table 1: Main particulars of RSL hull model

Main Particulars	Hull Spacing (m)		
	0.5	0.6	0.7
Length Overall (m)	0.733	0.820	0.906
Beam Overall (m)	0.620	0.720	0.820
Height (m)	0.325	0.325	0.325
Draft (m)	0.268	0.268	0.268
Wetted Surface Area (m <sup>2</sup> )	1.311	1.311	1.311

This concept is used to accomplish the design requirements related to the low drag and minimum power in operation. A control system needs to be developed and installed in order to enable self-manoeuvring by using specific controllers and sensors. The autonomous system needs to be developed using specific programming as a core of the self-manoeuvring vehicle [8]. Each hull will be put a motor thruster system at the bottom as propulsion system. This means the motor thruster functions as propulsion as well as steering system.

### 3.0 MODEL TEST

Model testing is an accurate and reliable method for measuring and investigating ship resistance. The model is designed down half scale of the prototype size. The design only consists of three fiberglass moulded hulls and one plywood as a platform, with four selected spacing between the three hulls which are placed in a triangle position. The selected spacing of the hull is 0.5m, 0.6m and 0.7m. Figure 2 shows an example of the distance between hulls which are represent by spacing of 0.7m. The size of the model was 0.7 m long, 0.85 m wide, and 0.4 m depth with a total weight of 18 kg.

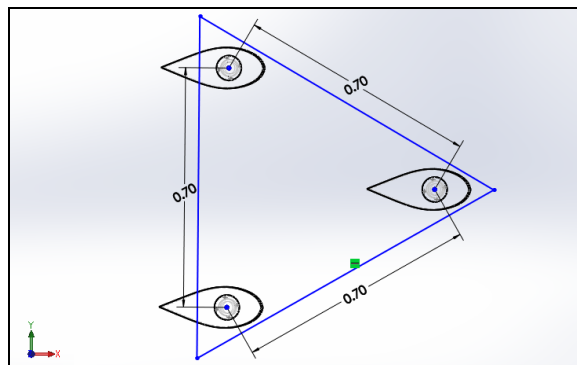


Figure 2: The hulls spacing of RSL model of the USV at spacing 0.7m.

The model tests were carried out to support the existing design work and validate numerical predictions of hull form resistance. In this study, the model tests were accomplished in a towing tank at the Southampton Solent University (SSU) Towing Tank (as shown in Figure 2), while the principal dimensions are summarised in Table 2. The experimental setup at the SSU towing tank consists of a single tow post dynamometer constraining the model in surge, sway, and yaw as shown in Figure 2. Through the tow post, the model was connected to the towing carriage which runs on rails during performing the tests.



Figure 3: Model tests at the Southampton Solent University (SSU) Towing Tank.

Table 2: Main Particulars of Southampton Solent University Towing Tank.

Main Particulars	Value
Length (m)	60.00
Breadth (m)	3.70
Depth (m)	1.85
Max. carriage speed ( $\text{ms}^{-1}$ )	4.50

The aims of the test are to measure the total resistance of the RSL model at five condition speeds and four location configurations of the hulls. The test was conducted in calm water. The model speed was set at 0.2 to 0.6  $\text{ms}^{-1}$  after extrapolating using Froude Scale. In order to guide the testing of the models to improve the test results, ITTC [9] recommended the ITTC procedures to be followed as closely as possible. The underwater cameras (as shown in Figure 4) were also used to record the movement of the model according to the test speed and get a visual of current flow on the submerged model body.



Figure 4 Visual of the submerged model bodies.

## 4.0 NUMERICAL SOLUTION

### 4.1 Mathematical Model

Viscous flow solver was used in this study for the simulation along with the Reynolds and Navier-Stokes (RANS) code to simulate the turbulent flow with the free surface effect based on the development of longitudinal vortices and on the viscous component of resistance. The equations of Navier-Stokes are the basic governing equations for a viscous, which is compressible actual fluid and it is a vector equation obtained by applying Newton's Law of Motion. Furthermore, it is also known as momentum equation

with the implementation of continuity equation and both of these equations are shown in Equation 1 and Equation 2 respectively.

$$\frac{\partial \rho}{\partial t} + \frac{\partial}{\partial x_j} [\rho u_j] = 0 \quad (1)$$

$$\frac{\partial}{\partial t} (\rho u_i) + \frac{\partial}{\partial x_j} (\rho u_i u_j + p \delta_{ij} - \tau_{ji}) = 0 \quad (2)$$

where,  $i = 1, 2, 3$

In order to predict the wave pattern, the free surface has to be simulated using the viscous code. In this study, the simulation was made by using interface-capturing method, Volume of Fluids (VOF), where this method is applied to assess free surface fluid motion in the simulation. Based on the concept of fractional volume of fluid Eulerian fixed-grid technique, the VOF can determine the shape and location of the free surface. Equation 3 shows the governing of this method.

$$\frac{DF}{Dt} = \frac{\partial F(\bar{x}, t)}{\partial t} + (\bar{V} \bullet \nabla) F(\bar{x}, t) = 0 \quad (3)$$

$F = 0$  : corresponds to any empty element occupied by no fluid

$F = 1$  : corresponds to a full element occupied by the fluid

$0 < F < 1$  : if cell contains the interface between the fluids

In addition, Shear Stress Transport (SST) turbulent model was used. The SST turbulence model is the combination of  $k-\epsilon$  model at the inner boundary and  $k-\omega$  model at the outer boundary [10] which has been implemented into Ansys CFX in order to achieve an optimal model formulation for a wide range of applications. As the concern on the accuracy at the boundary layer, this model is recommended in this study. Equation 4 shows the equation formulation used in the SST model.

$$\begin{aligned} \nabla \bullet (\rho U k) &= \nabla \bullet \left[ \left( \mu + \frac{\mu_t}{\sigma_{k3}} \right) \nabla k \right] + P_k - \beta' \rho k \omega \\ \nabla \bullet (\rho U \omega) &= \nabla \bullet \left[ \left( \mu + \frac{\mu_t}{\sigma_{\omega 3}} \right) \nabla \omega \right] + (1 - F_1) \rho \frac{2}{\sigma_{\omega 2} \omega} \nabla k \nabla \omega + \alpha_3 \frac{\omega}{k} P_k - \beta_3 \rho \omega_2 \end{aligned} \quad (4)$$

## 4.2 Computational Grid

Computational grid is an important matter that needs to be considered during performing CFD validation as to ensure the accuracy of the results. An unstructured mesh (tetrahedral) was employed by using Ansys ICEM around the free surface of the three-hull model of the RSL as shown in Figure 5 (a). Based on Figure 5 (b), the free surface and surface area of the three-hull RSL model were set to be prism.

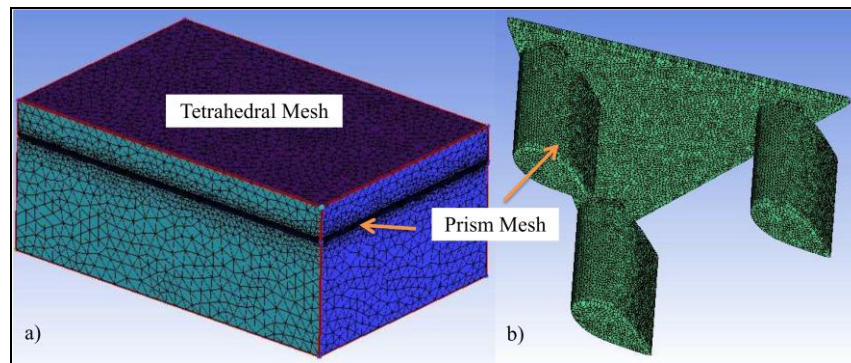


Figure 5: Meshing grids on domain and rudder shaped-like hull of USV model.

In this study, different meshing grids were used to study the grid independence on the configuration of 0.7 m RSL hull model. There are four cases of number of elements with different size of an element as shown in Table 3. This is a critical part in the simulation process as selecting number elements needs to be used for the simulation accuracy. The domain with higher number of elements may consume longer time to converge, while the domain with a smaller number of elements may affect the accuracy of the results [11].

**Table 3** Meshing info of USV model with spacing 0.7m at the speed of  $0.6 \text{ ms}^{-1}$ .

Study Case	Case 1	Case 2	Case 3	Case 4
Max. Element Size	0.42	0.36	0.30	0.27
No. of Elements	1.8m	2.5m	3.8m	4.8m
No. of Nodes	381k	544k	807k	990k

### 4.3 Domain And Boundary Conditions

The boundary condition and physical of the computational domain as shown in Figure 6 are both same for all of the configurations of the three RSL and cylindrical-columns model of the USVs. The total resistance calculated in this simulation is the sum of the pressure force and the friction force. Furthermore, the wave resistance is predicted from the pressure force obtained in the simulation because it is the sum of the viscous pressure force and wave force.

The inlet is set with defined volume fraction and turbulence intensity of 0.05, while the outlet is set as opening with entrainment and relative pressure is downstream pressure. Both inlet and outlet boundary was set as subsonic flow each. On the hulls surface, the boundary condition is defined as wall with no-slip condition. Then, for the both side of the domain including the top and base is defined as wall with free slip condition. The boundary conditions involved are as follows. The inlet boundary for the simulation is extends for  $1.50L$  in front of the model; outlet boundary is  $3.00L$  behind the model,  $1.85L$  to the port and starboard respectively and  $1.85L$  under the keel of the model. While for the air layer, its extend  $0.40L$  above the free surface.

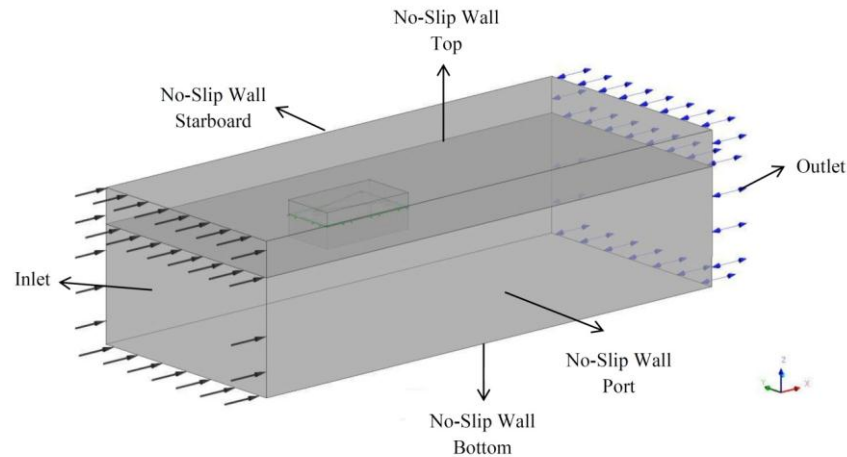


Figure 6: Computational domain of three RSL hulls model of the USV.

The inlet was set with defined volume fraction and turbulence intensity of 0.05, while the outlet was set as opening with entrainment and relative pressure as downstream pressure. Both inlet and outlet boundaries were set as subsonic flow each. On the surface of the hulls, the boundary condition is defined as wall with no-slip condition. Then, the both sides of the domain including the top and base are defined as wall with free slip condition. The boundary and physical condition of the computational domain are both similar for all configurations of the three RSL model. The total resistance calculated in this simulation is the sum of the pressure and friction forces. Furthermore, the wave resistance is predicted from the pressure force obtained in the simulation because it is the sum of the viscous pressure and wave forces. Then, after the simulation, the wave profile and pressure distribution contour will illustrate the wave pattern generated from the three-hull RSL model.

#### 4.4 CFX Solver

CFX is one of the software that is capable and familiar in calculating the ship resistance [4]. The problem in multiphase flow can be solved using turbulence model, the fluid region and different mesh style in this solver. For this study, the flow was considered as steady state in CFX calculations, and the finite volume method is used for the discretization process.

## 5.0 RESULTS AND DISCUSSION

### 5.1 Grid Independent Study

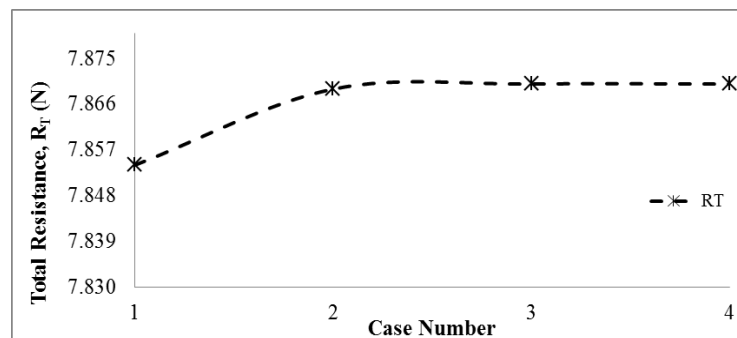


Figure 7: Grid independence study cases for RSL model with the configuration of 0.7 m at the speed of  $0.6 \text{ ms}^{-1}$ .

From the simulation by Ansys CFX, the results of the grid independent study were plotted as shown in Figure 7. It was found that the graph is gradually increase from case number 1 to case number 2 with numbers of elements 1.8 million and 2.5 million respectively. Then it was constant from case number 2 till case number 4. Thus, this indicates that this simulation has reached a solution value that is independent of the mesh resolution. For further analysis, the case 3 with 3.8 million numbers of elements were used. This is because, case number 3 is in between case number 2 and case number 4. Thus, this indicates that this meshing case have the capability to reduce the error. Even case number 4 which has more number of elements should act more dependent, but due to large number of elements, it may consume a lot of time to reach discretization.

## 5.2 Numerical Validation

Even though the grid independent study has been performed, it still requires the true value of the results from an experiment as to control the percentage of the relative errors. The true value was obtained by conducting the experiments, while the measured value was getting through the simulations. The results obtained from experimental and numerical studies of the RSL model between configuration 0.5, 0.6, and 0.7 m are compared as shown in Figures 8, 9, and 10. As a practice, the results from CFD analysis need to be validated by comparing them with the results of model tests in the preliminary step of ship design.

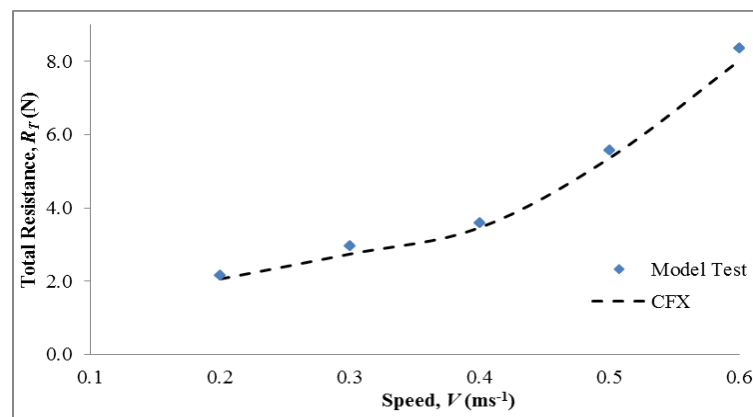


Figure 8: Comparison of total resistance RSL model between experiment and CFD test at 0.5 m configuration.

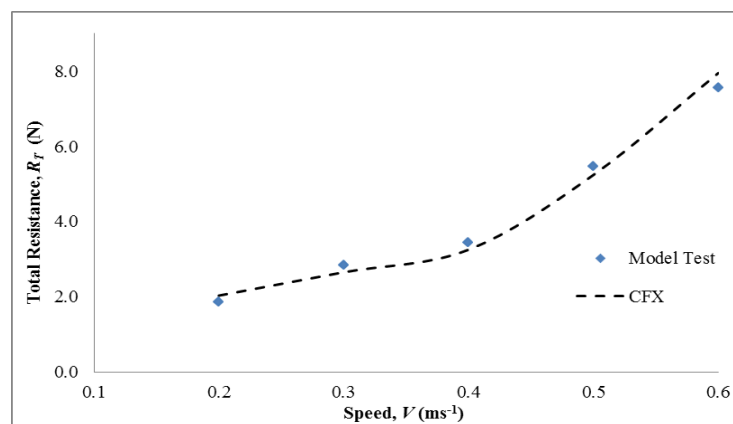


Figure 9: Comparison of total resistance RSL model between experiment and CFD test at 0.6m configuration.

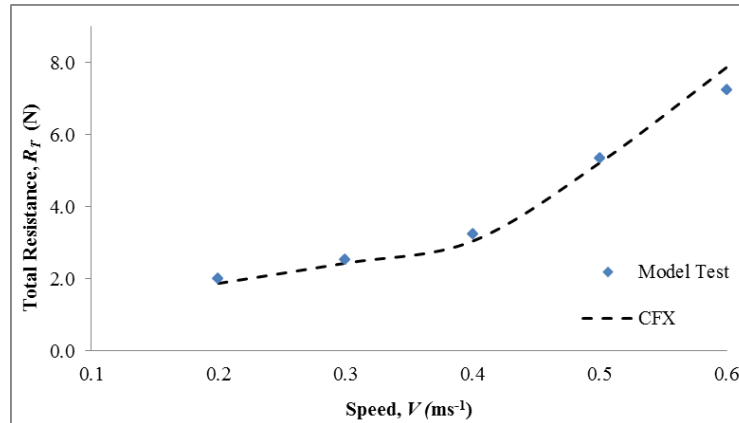


Figure 10: Comparison of total resistance RSL model between experiment and CFD test at 0.7 m configuration.

As shown in these figures, in all states, it was observed that numerical results are in good agreement with experimental results with the variation about 4 % to 9 %. This error can be due to the following reasons. The trim and sinkage of the model are kept fixed in CFD modeling, unlike the model test conditions. This may be the effect from the wave making and interference effect between the hulls that affect the total resistance of the model. Another reason may be due to the weakness of this CFD code for calculating wave making resistance.

### 5.3 Variation of Hulls Spacing

Figure 11 shows the comparison between the RSL model at different separation of hulls which are 0.5m, 0.6m and 0.7m. The graphs patterns are all the same where it is increase gradually from speed  $0.2 \text{ ms}^{-1}$  to speed  $0.4 \text{ ms}^{-1}$  before it is drastically increase from speed  $0.4 \text{ ms}^{-1}$  to  $0.6 \text{ ms}^{-1}$ . At low speed, the resistance was dominated by the viscous resistance before it is slowly dominates by wave making resistance as the speed increase as shown in Figure 12 and Figure 13 respectively..

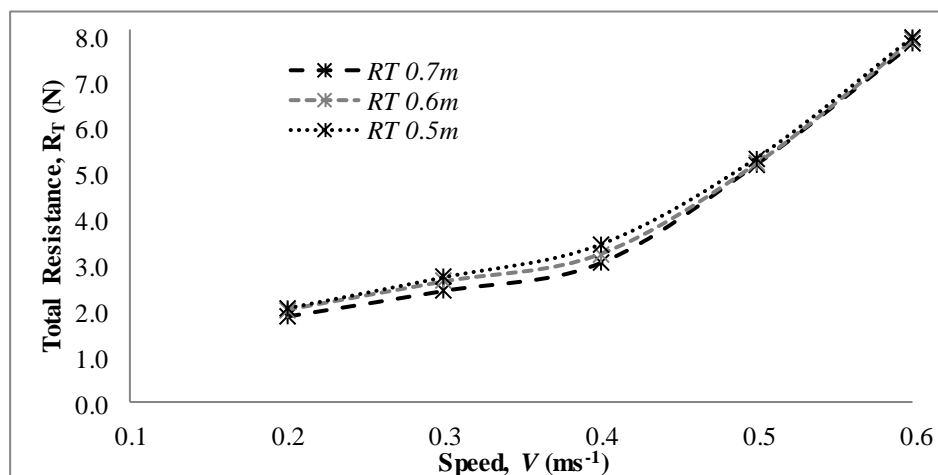


Figure 11: Total resistance of the model at spacing 0.5m, 0.6m and 0.7m.

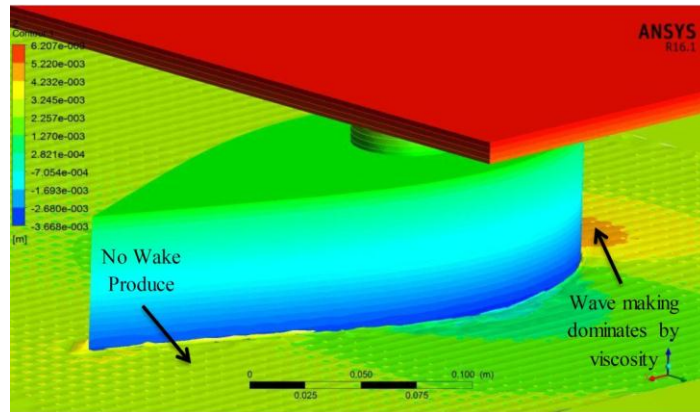


Figure 12: Free surface at hull speed,  $V = 0.2 \text{ ms}^{-1}$ .

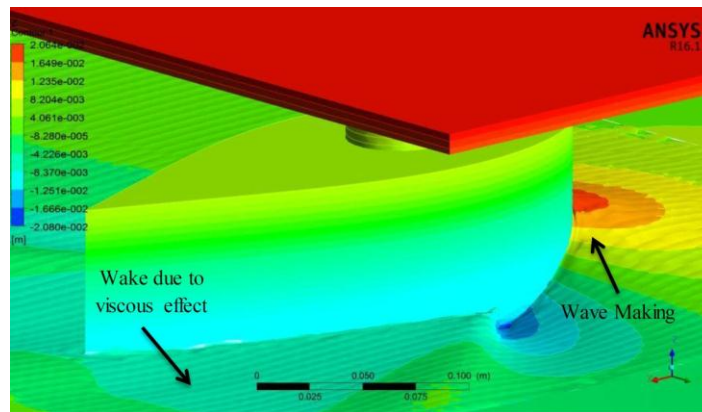


Figure 13: Free surface at hull speed,  $V = 0.6 \text{ ms}^{-1}$ .

In addition, by referring to Figure 11, it was found that the resistance decrease as the separation become wider. Comparison of the total resistance between speeds at  $0.2 \text{ ms}^{-1}$  to  $0.4 \text{ ms}^{-1}$  are quite bigger compared to the different at  $0.5 \text{ ms}^{-1}$  and  $0.6 \text{ ms}^{-1}$  which are much closer but still the resistance is decrease as the separation becomes wider. Even though the wetted surface of these three configurations is same, but the spacing are different thus affect the total resistance. The different of the results is due to the existing of the interference effect between the hulls which can be beneficial or harmful to the model. In other words, the interference effect is cause by the wave making resistance as shown in Figure 14 which is produce from the front hull which then interacts with the hull at the back. The interaction is different due to the different spacing thus affect the total resistance.

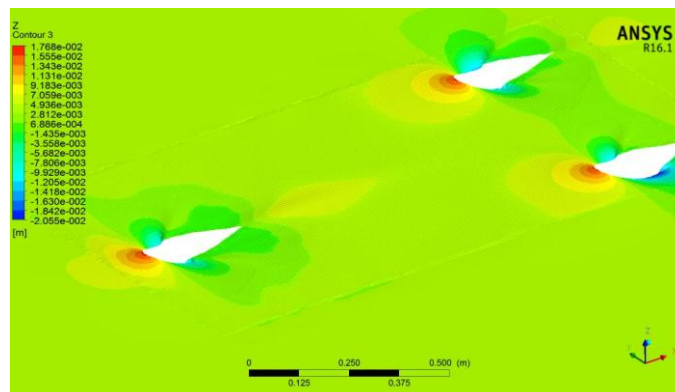


Figure 14: Free surface at hull speed,  $V = 0.6 \text{ ms}^{-1}$ .

## 6.0 CONCLUSIONS

By taking into account the general considerations in the ship design, a proper positioning of hulls in multi-hull configurations can bring significant benefits to hydrodynamic characteristics of the particulars on the ship resistance point of view. The experimental and numerical analysis using the results obtained from a RSL model shows that the position of the configurations on defined hulls has a significant effect on vessel motion characteristics.

It can be concluded that a larger configuration distance between three hulls leads to a reduction in resistance for identical hulls that have similar speed, and the resistance increases when the speed increases for all configurations of the three hulls. This result may help to accomplish the concept design required which is related to low-drag and minimum power operation.

Because of the complexity of the flow around the hull of the ship, model experiments are still the most reliable data source on ship resistance determination, so that a combined use of both model tests and CFD codes can be very useful for ship design and understanding the ship hydrodynamics. However, the simulation studies still lack support and verification from real experimental data. Furthermore, if the research is conducted using simulations and experiment, the results are validated with experimental data. The simulation results are in good agreement with the experimental data.

## ACKNOWLEDGEMENTS

We would like to acknowledge the reviewer(s) for the helpful advice and comments provided. The authors wish to thank the Research Management Center, UTM, for the financial support of this study through UTM Research University Grant (RUG) number Q.J130000.2524.06H08.

## REFERENCES

1. Azzeri, M. N., Adnan, F. A., Md Zain, M. Z. and Adi, M. (2016). *A Concept Design of Three Rudders-Shaped Like Body in Columns for Low-Drag USV*. International Conference on Innovative Research 2016 - ICIR Euroinvent 2016, Iasi, Romania, pp. 1-8: IOP Publishing.
2. Sahoo, P. K., Mynard, T., Mikkelsen, J. and McGreer, D. (2008). *Numerical and Experimental Study of Wave Resistance for Trimaran Hull Forms* HIPER '08 - The 6th International Conference on High-Performance Marine Vehicles, Naples, Italy, pp. 117-132.
3. Dubrovsky, V. (2004). *Ships with Outriggers*. Fair Lawn, USA,: Backbone Publishing
4. Ahmed, Y. M., Yaakob, O. B., Rashid, M. F. A., & Elbatran, A. H. (2015). Determining Ship Resistance Using Computational Fluid Dynamics (CFD). *Transport System Engineering, 1*, 20–25.
5. Salina, A., Goutam, K. S. and Md. Abdul, A. (2010). Drag Analysis of Different Ship Models using Computational Fluid Dynamics Tools. *The International Conference on Marine Technology*, Dhaka, Bangladesh.
6. Migali, A., Miranda, S. and Pensa, C. (2001). Experimental Study on the Efficiency of Trimaran Configuration for High-Speed Very Large Ship. *In Proceedings of the International Conference on Fast Sea Transportation FAST* Southampton, United Kingdom.
7. Hafez, K. A. (2012). Comparative Analysis of the Outriggers Immersion Influence on the Hydrodynamic Performance of High Speed Trimarans. *International Review of Mechanical Engineering* 6(7): 1559 - 1572

8. Azzeri, M. N., Adnan, F. A. and Md Zain, M. Z. (2015). Review of Course Keeping Control System for Unmanned Surface Vehicle. *Jurnal Teknologi*, 74 (5): 11-20.
9. ITTC. (2008). *Final report and recommendations to the 25th ITTC*. In: Proceedings of 25th international towing tank conference. Fukuoka, Japan.
10. Menter, F. R., Ferreira, J. C., & Esch, T. (2003). The SST Turbulence Model with Improved Wall Treatment for Heat Transfer Predictions in Gas Turbines. *International Gas Turbine Congress 2003*, (1992), 1–7.
11. Owen, S. (1998). A survey of unstructured mesh generation technology. *7th International Meshing Roundtable*, 25.